Determination of Vibrational Modes of L-Alanine Single Crystals by a Combination of Terahertz Spectroscopy Measurements and Density Functional Calculations

J. L. Allen,* T. J. Sanders, J. Horvat, and R. A. Lewis
Institute for Superconducting and Electronic Materials and School of Physics, University of Wollongong, Wollongong, New South Wales 2522, Australia

K. C. Rule
Australian Centre for Neutron Scattering, Australian Nuclear Science and Technology Organisation, Lucas Heights, New South Wales 2234, Australia

(Received 3 October 2022; accepted 17 March 2023; published 1 June 2023)

Density-functional theory may be used to predict both the frequency and the dipole moment of the fundamental oscillations of molecular crystals. Suitably polarized photons at those frequencies excite such oscillations. Thus, in principle, terahertz spectroscopy may confirm the calculated fundamental modes of amino acids. However, reports to date have multiple shortcomings: (a) material of uncertain purity and morphology and diluted in a binder material is employed; (b) consequently, vibrations along all crystal axes are excited simultaneously; (c) data are restricted to room temperature, where resonances are broad and the background dominant; and (d) comparison with theory has been unsatisfactory (in part because the theory assumes zero temperature). Here, we overcome all four obstacles, in reporting detailed low-temperature polarized THz spectra of single-crystal L-alanine, assigning vibrational modes using density-functional theory, and comparing the calculated dipole moment vector direction to the electric field polarization of the measured spectra. Our direct and detailed comparison of theory with experiment corrects previous mode assignments for L-alanine, and reveals unreported modes, previously obscured by closely spaced spectral absorptions. The fundamental modes are thereby determined.

DOI: 10.1103/PhysRevLett.130.226901

Alanine ($C_3H_7NO_2$) is an amino acid which occurs naturally in the human body. It is the simplest amino acid to demonstrate chirality. Alanine is one of the earliest amino acids, fundamental to early life for metabolic processes and protein formation [1,2]. In modern life, alanine is essential to many peptide and protein structures, whose hydrogen bonds and van der Waals interactions mediate essential biochemical functions. Recently, the simplest amino acid, glycine, has been found to form in interstellar space through a nonenergetic mechanism, and it is suspected that the next-simplest amino acid, alanine, may also [3]. L-Alanine forms a molecular crystal of space group $P2_12_12_1$. Each molecule is in a zwitterionic form, where the amine and carboxylic groups are ionized. As is evident in the molecular crystal structure shown in Fig. 1(a), this charge distribution gives rise to a dense and complex network of hydrogen bonds [4].

Low-energy hydrogen bonds, such as those which constitute crystalline L-alanine, are associated in energy with electromagnetic radiation in the terahertz (THz) region. For this reason, terahertz spectroscopy has served as an effective probe of the intermolecular interactions of a wide range of biomolecules [5–10] and pharmaceuticals [11,12] and is an appropriate technique to characterize the interactions in L-alanine. Terahertz spectroscopy has been used to assign vibrational modes, elucidate the mechanics of protein formation and function [13], and unravel molecular dynamics [14]. More generally, terahertz physics is an emerging field of wide application [15]. The terahertz roadmap [16] predicts numerous advances, which have recently spanned terahertz axions [17], metamaterials [18], and field-induced ferroelectricity [19].

Returning now to molecular crystals, the precise origins of the terahertz modes are poorly understood. They are usually inferred from the mode energy and crystal structure. In contrast to the bulk of experimental data reported, which does not use polarized radiation, polarized ("anisotropic") THz spectroscopy distinguishes vibrational modes with respect to crystal symmetry via the orientation of the dipole moments [20]. This technique also permits the observation of modes that would otherwise be obscured by closely spaced absorption bands [21,22]. Thus, polarized THz spectroscopy allows for a much more precise mode assignment, yielding better insight into the physical origin of the observed modes.

We now focus on L-alanine. While it has been intensely studied in the low-energy spectral region [7,10,23–32], many questions relating to its molecular dynamics are still to be answered with precision, due to inadequate theory and experiment. This is due to five main factors.

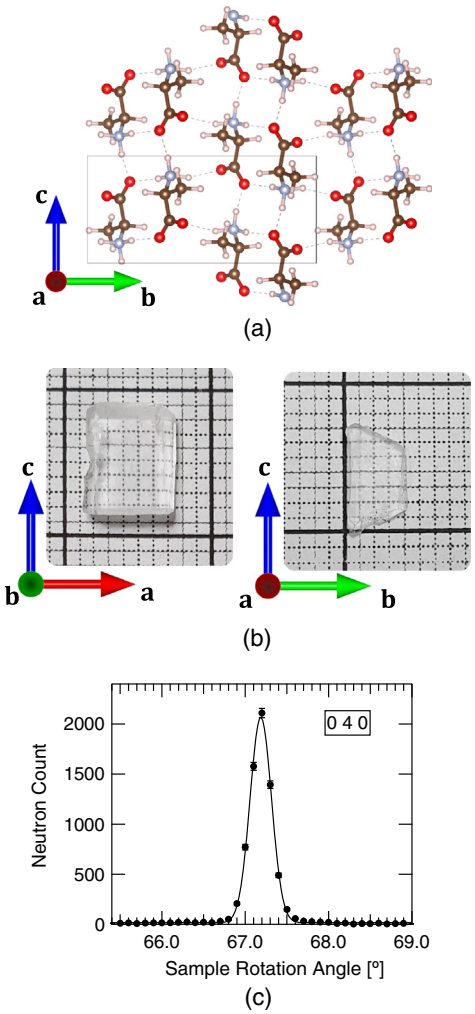

FIG. 1. (a) 1.5 × 2 unit cells of L-alanine. Dashed lines denote hydrogen bonds (threshold set to 2.10 Å). The box represents one unit cell. Structure from Lehmann *et al.* [4]. (b) L-Alanine single crystals. Left: with *c* axis vertical and *a* axis horizontal, used for *a*-axis and *c*-axis polarized synchrotron spectra. Right: with *c* axis vertical and *b* axis horizontal, used for *b*-axis polarized synchrotron spectra. Both are shown on a 1 cm grid. (c) The 0 4 0 reflection of a single crystal of L-alanine measured with 2.345 Å neutrons at ACNS using the Taipan thermal triple-axis spectrometer. The solid line is a Gaussian fit to the data. The narrow reflection peak indicates a high degree of monocrystallinity.

First, density-functional theory (DFT) calculations, while prolific [9,33–36], in many cases only agree poorly with experimental spectra. The difficulty may be often traced to the use of functionals that do not model intermolecular hydrogen bonds well. As mentioned above, such bonds are largely responsible for the low-energy vibrational modes in L-alanine. This issue has only recently been identified [37] and will be fully resolved here.

Secondly, the precise characterization of L-alanine in the terahertz region is hampered by the lack of high-quality samples. Previous studies have commonly used blends containing L-alanine in a binding medium for pellets [9,25,27]. The single-crystal approach of this work removes the potential of observing extrinsic features arising from the binder or interactions between the binding media and the material under study. Moreover, single crystals scatter less light than pellets.

Thirdly, the use of crystals permits the modes associated with different crystallographic axes to be excited by linearly polarized radiation. Polarized THz spectroscopy provides direct information to compare to DFT modeling concerning the dipole moment direction.

Fourthly, the polarized data allow us to separate modes which were previously obscured.

Fifthly, by measuring at low temperatures, where resonances are sharper, we have been able to observe previously unidentified modes with unparalleled clarity.

We now outline our theoretical approach. Further details are provided in the Supplemental Material [38]. DFT was used to calculate the vibrational modes in L-alanine. The CRYSTAL17 package was used [44]. Initial atomic coordinates from Lehmann *et al.* [4] were the seed for full geometric optimization of both atomic positions and the unit cell.

Zwitterionic amino acids have proven very difficult to model with DFT methods to the accuracy required for obtaining THz spectra comparable to experiment. Key to our modeling is the choice of an appropriate DFT functional. The B97-3c functional was chosen on three grounds: it includes an appropriate basis set, and is fast and accurate in modeling noncovalent interactions that are important for this crystal. The B97-3c functional has been successful in modeling other molecular crystals [45–47]. It uses van der Waals interactions, and short-range basis set corrections. Modified def2-TZVP basis sets (triple zeta valence basis set with new polarization functions) [48] are used, specifically mTZVP [48,49]. The B97-3c functional is a low-cost generalized gradient approximation (GGA) functional 2–3 times faster than the standard GGA functional when used with the mTZVP basis set. Even though faster, it has been shown to perform with an accuracy level better than the standard GGA functionals for light, main group elements [45].

Since accurate modeling of the experimental terahertz spectrum of L-alanine has proved to be difficult [9,33,50], very tight convergence criteria were employed for the full geometry optimization. The details are given in the Supplemental Material [38]. The infrared absorption spectrum was calculated in the harmonic approximation for the final converged geometry. The intensities of the absorptions were calculated with the Berry phase approach [51,52].

We now characterize the samples. Single crystals were grown using the solvent evaporation method [53]. The crystals used for measurements are shown in Fig. 1(b). Two crystals were used, one with an *a* face and one with a *b* face, to allow all three principal crystallographic axes to be probed. For optimum anisotropic measurements, it is best

to ensure that only one crystallographic axis is probed in any one measurement. Ideally the sample should be monocrystalline. The morphology of the samples was determined using elastic neutron scattering on the Taipan thermal triple-axis spectrometer [54] at the Australian Centre for Neutron Scattering (ACNS), and agrees with the accepted growth morphology [55]. In checking the orientation, the 0 4 0 reflection peaks in the L-alanine single crystals were found to have a low mosaic spread, of ∼0.8°, as may be seen in the sample rotation scan in Fig. 1(c). This is (only just) larger than the instrumental resolution of 0.66°. Figure 1(c) also indicates a good fit of the data to a Gaussian curve, which is expected for a crystalline reflection peak; moreover, there are no obvious additional peaks. This is also true for θ–2θ scans performed on the crystal samples. The same holds for the scans done on the 1 2 0 reflection peak (see also Fig. S1 [38]). The good Gaussian fits and the relatively narrow mosaic spreads suggest the samples are highly crystalline, and confirm that they are suitable for polarization measurements.

We now present our results. Anisotropic THz spectra of L-alanine were measured using synchrotron radiation at the Australian Synchrotron. The light was polarized using a rotatable wire-grid polarizer. The polarized experimental transmittance spectra of L-alanine are shown in Fig. 2. The *a*-axis and *c*-axis spectra were measured with the sample having the face perpendicular to the *b* axis [left-hand sample in Fig. 1(b)]. The *b*-axis spectrum was measured on the sample having the face perpendicular to the *a* axis [right-hand sample in Fig. 1(b)]. The frequency positions and absorbance intensities from our L-alanine DFT calculations are also shown on the same plots for electric dipoles excited by crystalline vibrations along the direction of each of the three axes.

The polarized spectra of L-alanine coincide well with the unpolarized spectrum (Fig. 2; also Fig. S3 and the discussion in Supplemental Material [38]). All features seen in the unpolarized spectrum appear distinctly in one of the polarized spectra. Furthermore, calculated modes from DFT also align well with the experimental spectra in Fig. 2, with the same number and approximately equivalent positions of the calculated modes and experimental absorption bands. Additionally, Fig. 3 (see also Figs. S5 and S6 [38]) shows the evolution of the experimental absorption bands as the incident polarization angle is varied. All absorption features fade systematically as the electric field polarization is rotated away from the axis along which the absorption is associated.

For the electric field of the THz radiation in the *a* direction, absorption bands are observed at 2.74, 3.12, and 3.26 THz, with a broad absorption band at 4.25 THz not completely resolved as it reaches the noise floor. These experimental results are in good agreement with the DFT calculation when the vibration-induced dipole moment direction is taken into consideration. For dipole moments along the *a* direction, DFT calculation predicts vibrational

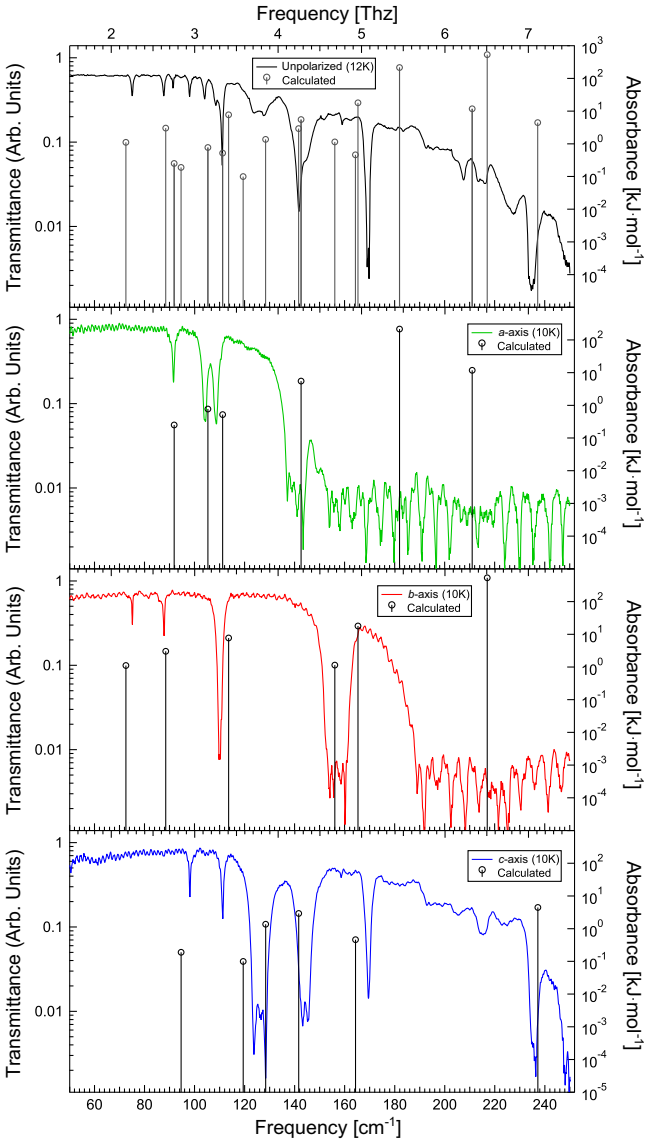

FIG. 2. Polarized THz measurements at 10 K along each crystallographic axis of L-alanine compared to DFT calculation mode positions for the *a* axis, *b* axis, and *c* axis, as well as the unpolarized spectrum at 12 K.

modes at 2.75, 3.16, 3.34, and 4.28 THz. Additional modes are calculated at 5.46 and 6.33 THz, beyond the experimental frequency cutoff of ≈4.5 THz.

In the *b* direction, absorption bands are observed at 2.25, 2.63, and 3.30 THz. A broad absorption appears at 4.71 THz and is absorptive enough to reach the noise floor. The observations agree with the DFT calculations of modes at 2.18, 2.65, 3.41, and 4.68 THz. A further mode is calculated at 4.96 THz. While not associable with an additional unique experimental absorption beyond that at 4.71 THz, it may be merged with the 4.71 THz absorption, given it is broad and it is incompletely resolved. An additional calculated mode at 6.51 THz lies above the cutoff frequency of the *b* axis polarization at 5.70 THz.

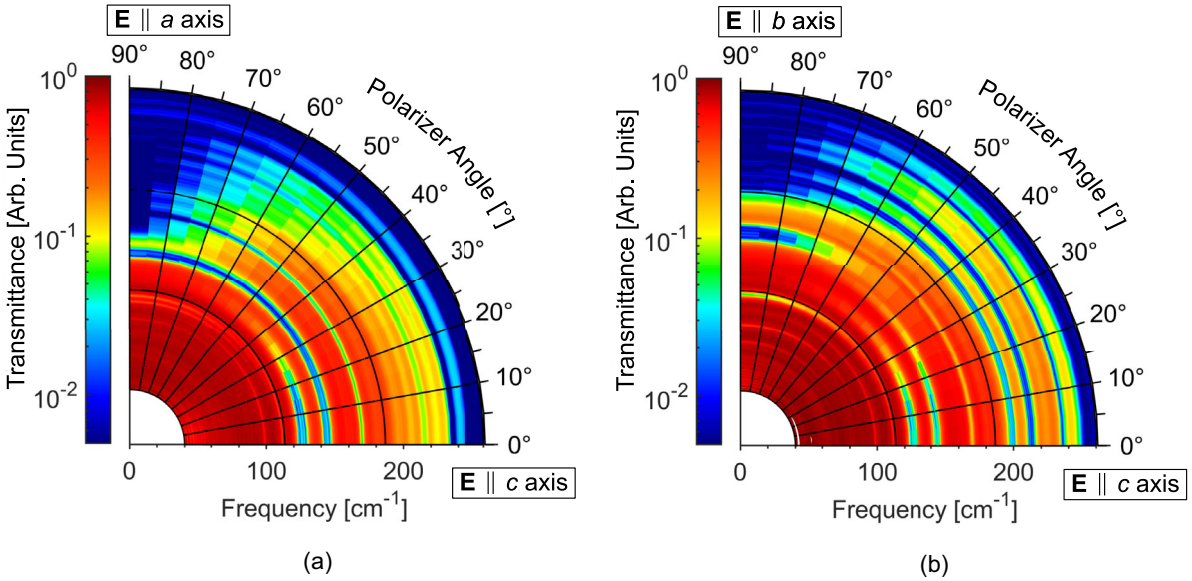

FIG. 3. Experimental polarized data at 7 K as the direction of $\vec{E}$ is varied. (a) a axis to c axis. (b) b axis to c axis. (The "heat map" format is to aid visualization. Conventional spectra appear in the Supplemental Material Figs. S5 and S6 [38]).

The c-direction polarization shows absorption bands at 2.94, 3.34, 3.79, 4.31, 5.08, 6.44, and 7.08 THz. DFT calculates modes at 2.84, 3.58, 3.85, 4.25, 4.93, and 7.11 THz. These are all in good agreement with the experimental absorptions, with the exception of the observed absorption at 6.44 THz. However, this feature does not have the same Lorenzian-like profile as the rest of the absorption bands assigned, and could reasonably be a nonresonant feature in origin. The frequency cutoff along the c axis is approximately 7.5 THz. The experimental and calculated modes along each axis are compared in Table I.

Previous work using unpolarized light [37] assigns the same DFT modes. However, it does so to different experimental modes in five cases, namely the 3.41, 3.58, 4.25, 4.28, and 4.96 THz modes. This clearly shows the improved reliability of studies using polarized spectra [38].

TABLE I. Observed absorption band positions along each crystallographic axis compared with the closest DFT calculated mode position. Modes are designated by frequency (in THz) with experimental modes at 10 K. Here, || denotes being parallel with respect to the incident electric field of the polarized light.

$\vec{E}\|a$ axis		$\vec{E}\|b$ axis		$\vec{E}\|c$ axis	
Experiment	DFT	Experiment	DFT	Experiment	DFT
2.74	2.75	2.25	2.18	2.94	2.84
3.12	3.16	2.63	2.65	3.34	3.58
3.26	3.34	3.30	3.41	3.79	3.85
4.25	4.28	4.71	4.68	4.31	4.25
	5.46		4.96	5.08	4.93
	6.33		6.51	6.44	
				7.08	7.11

An additional DFT mode at 7.11 THz is assigned here which was not presented in the earlier work [38].

As mentioned above, the polarization data exhibit frequency cutoffs of approximately 4.5 THz for the a axis, 5.7 THz for the b axis, and 7.5 THz for the c axis, which is the same for the anisotropic spectra. These results are consistent with and extend a previous report on the reflection THz spectrum of L-alanine [23] which shows strong, broad reflection beyond 4.8 THz perpendicular to the c axis, but no significant broad, intense reflections parallel to the c axis. Thus, it is not absorption, but rather strong reflection which most likely affects the frequency cutoff in the a and b directions.

In summary, our DFT modeling of dipoles excited along specific crystal directions agrees very well with our experimental polarization results. This lends confidence to the physical basis of the DFT calculations. Specifically, the success of the B97-3c functional in providing very accurate mode calculations has verified that weak hydrogen and van der Waals bonds are critical to the origin of the fundamental modes of L-alanine. Experimentally, through the use of polarized THz spectroscopy, closely spaced absorption bands have now been separated, confirming an additional mode at 3.30 THz (with a dipole moment along the b axis). Comparison with the DFT modeling has also extended the assignment of modes made in previous work [37]. Anisotropic theory combined with polarized experiments thus resolves the fundamental modes of L-alanine. Further refinement of the physical basis of the DFT functionals may yield even better agreement with the now robust experimental data.

This research used the THz/Far-IR beamline at the Australian Synchrotron and the Taipan thermal triple-axis

spectrometer at ACNS, both of which are a part of ANSTO, the Australian Nuclear Science and Technology Organisation. We thank D. Appadoo and R. Plathe for assistance. Numerical modeling was assisted by the National Computational Infrastructure (NCI), supported by the Australian Government. We thank AINSE Ltd. for financial assistance (Award-PGRA) to enable this research, also supported by Australian Research Council DP160101474.

*ja846@uowmail.edu.au

[1] P. G. Higgs and R. E. Pudritz, Astrobiology **9**, 483 2009).
[2] V. Kubyshkin and N. Budisa, Int. J. Mol. Sci. **20** (2019).
[3] S. Ioppolo, G. Fedoseev, K. Chuang, H. Cuppen, A. Clements, M. Jin, R. Garrod, D. Qasim, V. Kofman, E. van Dishoeck, and H. Linnartz, Nat. Astron. **5**, 197 (2021).
[4] M. S. Lehmann, T. F. Koetzle, and W. C. Hamilton, J. Am. Chem. Soc. **94**, 2657 (1972).
[5] T. Chen, Z. Li, and W. Mo, Spectrochim. Acta, Part A **106**, 48 (2013).
[6] T. Kleine-Ostmann, R. Wilk, F. Rutz, M. Koch, H. Niemann, B. Güttler, K. Brandhorst, and J. Grunenberg, ChemPhysChem **9**, 544 (2008).
[7] S. C. Shen, L. Santo, and L. Genzel, Int. J. Infrared Millimeter Waves **28**, 595 (2007).
[8] M. R. C. Williams, A. B. True, A. F. Izmaylov, T. A. French, K. Schroeck, and C. A. Schmuttenmaer, Phys. Chem. Chem. Phys. **13**, 11719 (2011).
[9] W. Yi, J. Yu, Y. Xu, F. Wang, Q. Yu, H. Sun, L. Xu, Y. Liu, and L. Jiang, Instrum. Sci. Technol. **45**, 423 (2017).
[10] W.-N. Wang, H.-Q. Li, Y. Zhang, and C.-L. Zhang, Acta Phys. Chim. Sin. **25**, 2074 (2009).
[11] L. M. Lepodise, Spectrochim. Acta, Part A **217**, 35 (2019).
[12] L. Xie, C. Wang, M. Chen, B.-B. Jin, R. Zhou, Y. Huang, S. Hameed, and Y. Ying, Spectrochim. Acta, Part A **222**, 117179 (2019).
[13] Y. He, P. I. Ku, J. R. Knab, J. Y. Chen, and A. G. Markelz, Phys. Rev. Lett. **101**, 178103 (2008).
[14] M. Hutereau, P. A. Banks, B. Slater, J. A. Zeitler, A. D. Bond, and M. T. Ruggiero, Phys. Rev. Lett. **125**, 103001 (2020).
[15] R. A. Lewis, *Terahertz Physics* (Cambridge University Press, Cambridge, United Kingdom, 2013).
[16] A. Leitenstorfer *et al.*, J. Phys. D **56**, 223001 (2023).
[17] J. Liu *et al.* (BREAD Collaboration), Phys. Rev. Lett. **128**, 131801 (2022).
[18] J. He, X. He, T. Dong, S. Wang, M. Fu, and Y. Zhang, J. Phys. D **55**, 123002 (2021).
[19] X. Li, T. Qiu, J. Zhang, E. Baldini, J. Lu, A. M. Rappe, and K. A. Nelson, Science **364**, 1079 (2019).
[20] H. Hoshina, Y. Morisawa, H. Sato, H. Minamide, I. Noda, Y. Ozaki, and C. Otani, Phys. Chem. Chem. Phys. **13**, 9173 (2011).
[21] Y. Deng, J. A. McKinney, D. K. George, K. A. Niessen, A. Sharma, and A. G. Markelz, ACS Photonics **8**, 658 (2021).
[22] R. Singh, D. K. George, J. B. Benedict, T. M. Korter, and A. G. Markelz, J. Phys. Chem. A **116**, 10359 (2012).
[23] Z. Mita, H. Watanabe, and S. Kimura, Infrared Phys. Technol. **96**, 7 (2019).
[24] N. Laman, S. Harsha, D. Grischkowsky, and J. S. Melinger, Biophys. J. **94**, 1010 (2008).
[25] Y. Liu, T. Zhou, and J.-C. Cao, Infrared Phys. Technol. **96**, 17 (2019).
[26] J. Darkwah, G. Smith, I. Ermolina, and M. Mueller-Holtz, Int. J. Pharm. **455**, 357 (2013).
[27] C. Ponseca, O. Kambara, S. Kawaguchi, K. Yamamoto, and K. Tominaga, J. Infrared, Millimeter, Terahertz Waves **31**, 799 (2010).
[28] A. R. Taulbee, J. A. Heuser, W. U. Spendel, and G. E. Pacey, Anal. Chem. **81**, 2664 (2009).
[29] J. Nishizawa, T. Sasaki, K. Suto, T. Tanabe, T. Yoshida, T. Kimura, and K. Saito, Int. J. Infrared Millimeter Waves **27**, 779 (2006).
[30] A. Matei, N. Drichko, B. Gompf, and M. Dressel, Chem. Phys. **316**, 61 (2005).
[31] M. Yamaguchi, F. Miyamaru, K. Yamamoto, M. Tani, and M. Hangyo, Appl. Phys. Lett. **86**, 053903 (2005).
[32] M. Barthes, A. F. Vik, A. Spire, H. N. Bordallo, and J. Eckert, J. Phys. Chem. A **106**, 5230 (2002).
[33] L. Jiang, J. Yu, C. Li, W. Yi, Y. Xu, and Y. Liu, in *Proceedings of the 2016 41st International Conference on Infrared, Millimeter, and Terahertz waves (IRMMW-THz)* (IEEE, Copenhagen, Denmark, 2016), pp. 1–2, 10.1109/IRMMW-THz.2016.7758446.
[34] W. Guo and W. Wei-Ning, Acta Phys. Chim. Sin. **28**, 1579 (2012).
[35] Z.-P. Zheng and W. Fan, J. Biol. Phys. **38**, 405 (2012).
[36] F. Zhang, H.-W. Wang, K. Tominaga, and M. Hayashi, J. Phys. Chem. A **119**, 3008 (2015).
[37] T. J. Sanders, J. L. Allen, J. Horvat, and R. A. Lewis, J. Chem. Phys. **154**, 244311 (2021).
[38] See Supplemental Material at http://link.aps.org/supplemental/10.1103/PhysRevLett.130.226901, for details of the calculated modes, further theoretical considerations, triple-axis neutron scattering for the 1 2 0 reflection, THz instrumentation, a comparison to the unpolarized spectrum, a comparison of *c*-axis spectra, and the comprehenive set of anisotropic spectra. Includes Refs. [39–43].
[39] F. Akhtar and J. Podder, Res. J. Phys. **6**, 31 (2012).
[40] T. J. Sanders, J. L. Allen, J. Horvat, and R. A. Lewis, Phys. Chem. Chem. Phys. **23**, 657 (2021).
[41] J. L. Allen, T. J. Sanders, R. Plathe, D. Appadoo, J. Horvat, and R. A. Lewis, Spectrochim. Acta, Part A **260**, 119922 (2021).
[42] J. L. Allen, T. J. Sanders, J. Horvat, and R. A. Lewis, Spectrochim. Acta, Part A **244**, 118635 (2021).
[43] T. J. Sanders, J. L. Allen, R. Plathe, D. Appadoo, J. Horvat, and R. A. Lewis, Spectrochim. Acta, Part A **286**, 121970 (2023).
[44] R. Dovesi, A. Erba, R. Orlando, C. M. Zicovich-Wilson, B. Civalleri, L. Maschio, M. Rérat, S. Casassa, J. Baima, S. Salustro, and B. Kirtman, WIREs Comput. Mol. Sci. **8**, e1360 (2018).
[45] J. G. Brandenburg, C. Bannwarth, A. Hansen, and S. Grimme, J. Chem. Phys. **148**, 064104 (2018).
[46] S. Grimme, J. Antony, S. Ehrlich, and H. Krieg, J. Chem. Phys. **132**, 154104 (2010).

[47] S. A. Katsyuba, E. E. Zvereva, and S. Grimme, J. Phys. Chem. A **123**, 3802 (2019).
[48] F. Weigend and R. Ahlrichs, Phys. Chem. Chem. Phys. **7**, 3297 (2005).
[49] S. Grimme, J. G. Brandenburg, C. Bannwarth, and A. Hansen, J. Chem. Phys. **143**, 054107 (2015).
[50] P. R. Tulip and S. J. Clark, J. Chem. Phys. **121**, 5201 (2004).
[51] F. Pascale, C. M. Zicovich-Wilson, F. López Gejo, B. Civalleri, R. Orlando, and R. Dovesi, J. Comput. Chem. **25**, 888 (2004).
[52] C. M. Zicovich-Wilson, F. Pascale, C. Roetti, V. R. Saunders, R. Orlando, and R. Dovesi, J. Comput. Chem. **25**, 1873 (2004).
[53] T. P. Srinivasan, R. Indirajith, and R. Gopalakrishnan, J. Cryst. Growth **318**, 762 (2011).
[54] S. A. Danilkin and M. Yethiraj, Neutron News **20**, 37 (2009).
[55] F. Massimino, M. Bruno, M. Rubbo, and D. Aquilano, Cryst. Res. Technol. **46**, 789 (2011).